THE PENNSYLVANIA STATE UNIVERSITY
SCHREYER HONORS COLLEGE

DEPARTMENT OF BIOLOGY

Mitonuclear Conflict in the F1 Hybrid Coral '*Acropora prolifera*'

BRYAN MANZANO
SPRING 2023

A thesis
submitted in partial fulfillment
of the requirements
for a baccalaureate degree
in Biology
with honors in Biology

Reviewed and approved* by the following:

Illiana Baums
Professor of Biology
Thesis Supervisor

Benoit Dayrat
Professor of Biology
Honors Advisor

* Electronic approvals are on file.

ABSTRACT

The Caribbean's two most important reef building corals, elkhorn coral (*Acropora palmata*) and staghorn coral (*A. cervicornis*), cross to form the first generation (F1) hybrid coral "*A. prolifera"*. This F1 hybrid could mitigate damages to reefs due to elevated temperatures from climate change. One problem with using this hybrid coral within a conservation context is the potential for hybrid breakdown in later generations. In fact, "*A. prolifera"* is thought to be sterile since F2 hybrids of "*A. prolifera*" are not found on the reef. One mechanism leading to hybrid breakdown is termed mitonuclear conflict, where incompatibility between mitochondrially-encoded genes and nuclear-encoded genes negatively impact oxidative phosphorylation, limit efficient mitochondrial function, and lead to apoptosis. In this study, it was hypothesized that mitonuclear conflict causes hybrid breakdown in the F2 generation. A co-expression network analysis approach was used to test if mtDNA genes in the hybrid are differentially coexpressed when compared to its parental taxa, the result of which would suggest that the hybrid could have an altered oxidative phosphorylation (OXPHOS) pathway and thus experience mitonuclear conflict and hybrid breakdown. In this experiment, four genets of each taxon were collected in Belize and transferred to an in situ common garden. After six months, samples were taken and their RNA was sequenced. It was found that mtDNA genes were not tightly coexpressed as suggested by low values of a measure known as topological overlap measure, a finding that is contradictory to the normally rigid co-expression of critical mtDNA in the OXPHOS pathway. Clustering analyses also suggested that all mtDNA genes differed in co-expression, a finding that contradicts other studies. These results could be explained by technical errors during data analysis. Alternatively, *A. palmata* may have been stressed in the common garden environment and thus had altered gene expression leading to a disruption in the co-expression of mtDNA

genes. Additional analyses are required to distinguish between these possibilities before mitonuclear conflict can be ruled out as a cause of acroporid coral hybrid breakdown in F2 and later generations in the wild.

TABLE OF CONTENTS

LIST OF FIGURES iv

LIST OF TABLES v

ACKNOWLEDGEMENTS vi

Chapter 1 Introduction 1

Chapter 2 Materials and Methods 5

Chapter 3 Results 7

Chapter 4 Discussion 18

Appendix A Supplemental Information, Figures, and Tables 23

LIST OF FIGURES

Figure 1: Heatmap of mitochondrially encoded genes from DEseq2 analysis. Heatmap shows Z-scores of the rlog transformed expression data from the DEseq dataset by gene. Hierarchical clustering is shown both by genet (PJ = palmata, CJ = cervicornis, HJ = hybrid) and by gene.10

Figure 2: Clustering dendrogram of genes in the pre-control and pre-treatment *A. palmata* gene co-expression network (N = 7). Dissimilarity calculated using topological overlap measure (TOM). Module colors show the assigned module of each gene. 10

Figure 3: Clustering dendrogram of genes in the pre-control and pre-treatment *A. cervicornis* gene co-expression network (N = 7). Dissimilarity calculated using topological overlap measure (TOM). Module colors show the assigned module of each gene. 11

Figure 4: Clustering dendrogram of genes in the pre-control and pre-treatment *"A. prolifera"* gene co-expression network (N = 7). Dissimilarity calculated using topological overlap measure (TOM). Module colors show the assigned module of each gene.....11

Figure 5: *A. palmata* mtDNA network (N = 13, E = 16), with edges showing topological overlap measure between mtDNA genes (TOM > 0.02), with color gradient showing TOM range of 0.020-0.261. 13

Figure 6: *A. cervicornis* mtDNA network (N = 13, E = 31), with edges showing TOM between mtDNA genes (TOM > 0.02), with color gradient showing TOM range of 0.025-0.219. 13

Figure 7: *"A. prolifera"* mtDNA network (N = 13, E = 39) with edges showing TOM between mtDNA genes (TOM > 0.02), with color gradient showing TOM range of 0.020-0.141. 14

Figure 8: *A. palmata* mtDNA network (N = 14, E = 22) with edges showing TOM between mtDNA genes with decreased threshold (TOM > 0.01), with color gradient showing TOM range 0.011-0.261. Dotted edges were present when TOM threshold was 0.02, and solid blue edges were observed after the threshold decrease (TOM range 0.011-0.016). Nodes in yellow were seen after decreasing the threshold. 14

LIST OF TABLES

Table 1: Dataset sample information, showing sample ID (CJ = *A. cervicornis*, PJ = *A. palmata*, HJ = hybrid) genotype of each sample, taxon, timepoint (all have time point before exposure to treatment), treatment, and depth of common garden (approximately 4 meters). 8

Table 2: Table showing edge weights (TOM) for *A. cervicornis* between mtDNA genes. 15

Table 3: Table showing edge weights (TOM) for *A. palmata* between mtDNA genes. 15

Table 4: Table showing edge weights (TOM) for *"A. prolifera"* between mtDNA genes 16

ACKNOWLEDGEMENTS

I would like to thank Dr. Iliana Baums for advising this research along with C. Cornelia Osborne for her stellar mentorship and upstream preparation of the dataset. I would also like to thank Drs. Kelly Gomez-Campo and Sheila Kitchen for their network expertise.

Chapter 1

Introduction

Elkhorn coral (*Acropora palmata*) and Staghorn coral (*A. cervicornis*) breed naturally to form an F1 hybrid, "*A. prolifera*" that exhibits F2 hybrid breakdown (Vollmer & Palumbi, 2002). Historically, these two branching corals were the most prevalent reef-building taxa in the Caribbean, while their hybrid was not as prevalent (Vollmer & Palumbi, 2002). However, there has been an increase in hybrid abundance throughout the Caribbean, especially in Florida (Wheaton et al., 2006), Curacao (Fogarty, 2010), Honduras (Keck et al., 2005), the Lesser Antilles (Japaud et al., 2014), and Belize (Fogarty, 2010; Fogarty et al., 2012; Richards & Hobbs, 2015). These hybrid populations are capable of reproduction, with backcrossing known to occur to both parental species (van Oppen et al., 2002); however, there is likely some type of post-fertilization hybrid breakdown that prevents successful F2 hybrids from being produced, as no secondary generation hybrids have been found (Vollmer & Palumbi, 2002). In other well studied hybridizing species like the intertidal copepod (*Trigriopus californicus*), reproductive barriers were absent and F2 hybrids were found to be inviable due to mitonuclear conflict (Ellison & Burton, 2010). Such similarities to the coral hybrid system suggests that mitonuclear conflict should also be investigated as the driver behind *"A. prolifera"* hybrid breakdown.

Mitonuclear conflict happens when a mitochondrial gene from one species is placed in the nuclear genetic background of a differing species due to a hybridization event. This is possible because the mitochondrial genome is distinct from the nuclear genome in how it originated, evolved, and is passed on as explained by the endosymbiont theory (Sagan, 1967).

This separation of genomes allows for the possibility of each species in a hybrid system to have a distinct nuclear and mitochondrial genetic background. These backgrounds are distinct since over time, as each species' mitochondrial genome accumulates unique mutations, the nuclear genome of each species must evolve in an arms race to ensure it is able to produce proteins that work efficiently with altered protein products of the mitochondrial genome (Chou & Leu, 2015). It is when the nuclear genome is unable to evolve in pace with the mitochondrial genome that conflict arises, leading to hybrid breakdown (Burton et al., 2013).

In anisogamous acroporid corals that produce larvae via the fusion of egg and sperm, the nuclear genome is passed on by both parents and is subject to recombination, while the mitochondrial genome is inherited uniparentally from the female parent during sexual reproduction. This uniparental inheritance in theory leaves the mitochondrial genome vulnerable to the accumulation of deleterious mutations, otherwise known as Muller's Rachet (Chou & Leu, 2015), which forces the nuclear genome to evolve in an evolutionary arms race as previously mentioned. For example, if two coral populations are separated, each population's mitochondrial genome theoretically will accumulate deleterious mutations, and their respective nuclear genomes will coevolve to ensure proper mitochondrial function. This could lead to speciation, and if these species would then hybridize, offspring with the nuclear genetic background of one parent and the mitochondrial genetic background of the other would experience mitonuclear conflict.

This mitonuclear conflict can result in F2 hybrid breakdown due specifically to alterations in the oxidative phosphorylation pathway (Hill, 2015), which includes 13 critical mitochondrially encoded genes (MT-ATP8, MT-ATP6, MT-COX1, MT-COX2, MT-COX3, MT-CYB, MT-ND1, MT-ND2, MT-ND3, MT-ND4, MT-ND4L, MT-ND5, MT-ND6). Slightly

altering the interaction between the nuclear-encoded genes and these mitochondrial-encoded protein subunits making up complexes I-V of the electron transport chain can dramatically alter oxidative phosphorylation (OXPHOS) function (Hill, 2015). This alteration of the OXPHOS function again is the result of a disruption of coordinated expression between the nuclear genome and the mitochondrial genome.

More specifically, these 13 mitochondrially-encoded proteins make up important parts of complexes I, III, IV, and V of the electron transport chain (Hill, 2017). These 13 mt-encoded proteins also work directly with about 75 nuclear encoded proteins to form these important complexes (Burton & Barreto, 2013). Mt-encoded proteins and nuclear-encoded proteins work together to ensure efficient transfer of electrons along the electron chain and couple that with ATP production (Lane, 2011). Proper functioning of this pathway ensures adequate energy supply for both individual eukaryotic cells and whole organisms (Wallace, 2007). Alteration of this function puts constraints on the efficiency of ATP production in mitochondria and could result in eventual apoptosis for individual cells as well as have impacts on the survival of whole organisms (Hill, 2016; Burton et al., 2006).

Limited studies have investigated mitonuclear conflict in natural populations of animals like corals (Lee-Yaw et al., 2014; Rank et al., 2020; Ding et al., 2021). Because selectively breeding specific hybrid individuals is not possible given a natural population, differential gene expression analysis and gene ontology enrichment analysis have been alternatively used to show that mitonuclear mismatch arising from introgression can have fitness consequences, suggesting evidence of mitonuclear conflict as a driver of population divergence (Ding et al., 2021). In addition, Weighted Gene Correlation Network Analysis (WGCNA) using mtDNA expression as a correlated trait has also been used to build a mitonuclear co-expression network to correlate

genes and modules (Wang et al., 2014). It also should be noted that the 13 mitochondrially-encoded genes should by highly co-expressed with each other, as seen in previous studies using WGCNA to build mtDNA networks (Yuan et al., 2020). In this study, we consider that natural *A. palmata* x *A. cervicornis* hybrids could have signs of mitonuclear conflict as a result of this hybridization event.

The objective of this project is to investigate the presence of mitonuclear conflict in the coral hybrid "*A. prolifera"*. To test if mitonuclear conflict is a contributing factor to F2 hybrid breakdown in *"A. prolifera"*, co-expression network analyses will be used to analyze co-expression among the 13 protein-coding genes in the mitochondrial genome. Mitonuclear conflict would be indicated by mitochondrially-encoded genes being co-expressed differently among the three taxa. WGCNA will be applied to compare individually constructed co-expression networks for *"A. prolifera"* and its two parental taxa to identify disrupted co-expression among mitochondrial genes. This will be done first by identifying co-expression among the 13 mitochondrially genes using Topological Overlap Measure (TOM) to assess whether these genes are strongly interconnected based on a threshold TOM > 0.02 (Langfelder & Horvath, 2018). Further clustering analysis will be done by finding modules of interconnected genes and finding modules containing the 13 protein coding genes that are mitochondrially-encoded. Within the modules of interest, module membership (MM) will be ranked and differences in MM of genes in the OXPHOS pathway will be compared between the taxa. If no significant topological difference is found between modules containing mitonuclear genes, then no evidence for mitonuclear conflict will be present, leading to a conclusion that mitonuclear conflict does not impact F2 hybrid generation and other future offspring production.

Chapter 2

Materials and Methods

Background on Dataset:

The dataset used for this project was generated by C. Cornelia Osborne (PSU) in collaboration with Nikki Fogarty (UNCW) and Iliana Baums (PSU); briefly, in 2018, four genets of each of the three taxa were placed in a common garden environment using coral trees at Carrie Bow Cay Field, Belize for 6 months, then moved onshore for exposure to a heat stress experiment. The objective of this research was to find the genetic and physiological traits associated with each taxon when exposed to high temperature conditions, and to measure the hybrid's response relative to that of the parental species. Each genet was fragmented, with one fragment clone placed in a control temperature tank (28 ºC) and the other fragment placed in an experimental/treatment tank, with tissue samples taken from fragments before temperature increase. Samples before and after the experiment were processed for RNA extraction, and RNA sequencing via 3'-TAGseq. Transcriptomes were assembled for each of the three taxa, and TAGseq reads were aligned to both their respective transcriptomes, and to the *A. palmata* transcriptome. Transcriptomes were annotated per custom script by Osborne, 2023. Genets sampled prior to temperature ramp-up were used in this analysis, with biological replication captured by using both pre-treatment and pre-ambient exposed samples. More specifically, 8 samples total were used for *A. palmata* (4 pre-control, 4 pre-treatment, with each genet being exposed to both conditions), 7 samples total were used for *A. cervicornis* (4 pre-control, 3 pre-treatment, with each genet being exposed to both conditions except "Dale" genet), and 7 samples were used for *"A. prolifera"* (4 pre-control, 3 pre-treatment, with each genet being exposed to both conditions except "H112" genet). Since within-species differences in gene expression are

expected to be much less than between-species differences, the fact that we are using technical replicates here should not matter in downstream analyses. Gene counts were derived from alignment of TagSeq reads to the *A. palmata* reference transcriptome. The aforementioned custom perl script failed to align Tag-seq reads to the mitochondrial genome (Kitchen et al., 2021), necessitating an additional alignment step specifically for this project, using Kallisto to derive counts for the mitochondrial genes (Bray et al., 2016). All RNA extractions, sequencing, transcriptome assemblies, alignments, gene counts, and upstream analyses were done by C. Cornelia Osborne, 2023 (manuscript in prep.)

Differential Expression Analysis:

Differential gene expression was performed with DEseq2 v. 1.34.0 fitting the model ~ Species (Love et al., 2014). Regularized log (rlog) transformation was performed on the results from DEseq2, and pheatmap v. 1.0.12 was used to generate a heat map that show the Z-scores of the rlog transformed expression data from the DEseq dataset by gene. One heatmap was generated to show how mtDNA was expressed in each genet of the three taxa.

WGCNA network construction and module detection

WGCNA v. 1.70.3 (see Appendix A) was used to construct separate networks for *A. palmata*, *A. cervicornis*, and *"A. prolifera"* (Langfelder & Hovarth, 2008). Data was normalized before feeding into WGCNA using DEseq2. Soft-thresholding powers were chosen using a scale-free topology model (Langfelder & Hovarth, 2008). The powers 16, 14, and 22 were used for *A. palmata*, *A. cervicornis*, and *"A. prolifera"* network construction respectively (see Supplemental Figures 1-3). Automatic, one-step network construction and module detection were used for each network (see supplemental information).

Cytoscape analysis

Networks containing just the mtDNA genes were constructed in cytoscape for all three taxa with nodes representing the mtDNA genes and the edges representing topological overlap measure (Shannon et al., 2003; see supplemental information). A cutoff TOM > 0.02, the default threshold recommended by other studies (Langfelder & Hovarth, 2008) was used to generate edge files for this analysis. To determine the effect of TOM cutoff threshold on hub gene connectivity, a cutoff TOM > 0.01 was also used to build a second *A. palmata* mtDNA co-expression network.

Module membership ranking

Modules detected in each network can be ranked using a measure called Module membership (MM) in order to identify hub genes within each module that are highly connected to other genes in the module. MM is a correlation of gene expression profile to module eigengene that is representative of the gene expression profiles of genes in a given module, which gives back a value between -1 and 1. As it approaches 1, it means the given gene is more and more highly connected to other genes in the given module which are represented with the module Eigengene (Langfelder & Horvath, 2008). In this initial analysis, the top 10 genes based on MM were extracted from the modules of all three taxa that contained the mtDNA genes.

Chapter 3

Results

The dataset consisted of 4 genets (1-2 replicates per genet) from each taxon (Table 1). They were transferred from their natal reef (at depths varying from 0.7-14m) to a common garden environment at a depth of 4, where they were acclimated for 6 months. Transcript levels

of 13 mtDNA genes were extracted for each sample and used to construct gene expression networks. When running WGCNA with 8 samples of *A. palmata*, 7 samples for *A. cervicornis*, and 7 samples for *"A. prolifera"*, there were 51 modules, 39 modules, and 38 modules detected respectively. When one sample was cut from A. *palmata*, a total of 39 modules was detected for the construction, confirming that the number of modules for the three taxa was determined at least in part by the number of samples analyzed. This decrease in the number of modules for *A. palmata* was true regardless of which genet was removed from the dataset. Considering that significant module reduction was observed when all three network constructions were run with only 4 pre-control samples, cutting a random sample from the *A. palmata* dataset (sample 3236_PJ.counts which is a pre-treatment sample of the genet "P3011") was justified as the number of detected modules is directly related to sample size.

Table 1: Dataset sample information, showing sample ID (CJ = *A. cervicornis*, PJ = *A. palmata*, HJ = hybrid) genotype of each sample, taxon, timepoint (all have time point before exposure to treatment), treatment, and depth of common garden (approximately 4 meters).

Sample_ID	Genotype	Taxon	Timepoint	Treatment	Depth (m)
3122_CJ.counts	LBHK	*A.cervicornis*	Pre	Control	4
3234_CJ.counts	88	*A.cervicornis*	Pre	Control	4
3266_CJ.counts	LBHK	*A.cervicornis*	Pre	Treated	4
3267_CJ.counts	88	*A.cervicornis*	Pre	Treated	4
3272_CJ.counts	LBWR	*A.cervicornis*	Pre	Control	4
3277_CJ.counts	LBWR	*A.cervicornis*	Pre	Treated	4
3289_CJ.counts	Dale	*A.cervicornis*	Pre	Control	4
3042_PJ.counts	401	*A.palmata*	Pre	Treated	4
3138_PJ.counts	401	*A.palmata*	Pre	Control	4
3176_PJ.counts	P3014	*A.palmata*	Pre	Treated	4
3191_PJ.counts	P3014	*A.palmata*	Pre	Control	4
3211_PJ.counts	P3011	*A.palmata*	Pre	Control	4
3212_PJ.counts	96	*A.palmata*	Pre	Treated	4
3217_PJ.counts	96	*A.palmata*	Pre	Control	4
3236_PJ.counts	P3011	*A.palmata*	Pre	Treated	4

3118_HJ.counts	LBFL	*"A.prolifera"*	Pre	Control	4
3157_HJ.counts	H112	*"A.prolifera"*	Pre	Control	4
3181_HJ.counts	H13	*"A.prolifera"*	Pre	Treated	4
3200_HJ.counts	LBFL	*"A.prolifera"*	Pre	Treated	4
3246_HJ.counts	H13	*"A.prolifera"*	Pre	Control	4
3260_HJ.counts	H72	*"A.prolifera"*	Pre	Control	4
3283_HJ.counts	H72	*"A.prolifera"*	Pre	Treated	4

.

No clear hierarchal clustering by taxon was seen among the mtDNA genes (Figure 1). For example, 2 samples of *Acropora cervicornis* (3234_CJ.counts and 3267_CJ.counts) and 2 samples of *"A. prolifera"* (3118_HJ.counts and 3283_HJ.counts) show overall downregulation of mtDNA genes while another hybrid sample (3200_HJ.counts) exhibits overall upregulation of mtDNA genes (Figure 1). Thus, there is significant variation in expression between genets without respect to taxon.

The *A. palmata* gene co-expression network features a total of 39 modules, with the largest module having 7560 genes and the smallest having 94 genes (Figure 2). The *A. cervicornis* gene co-expression network features a total of 38 modules, with the largest module having 9699 genes and the smallest having 40 genes (Figure 3). The *"A. prolifera"* network features 39 detected modules, with the largest having 8719 genes and the smallest having 52 genes (Figure 4).

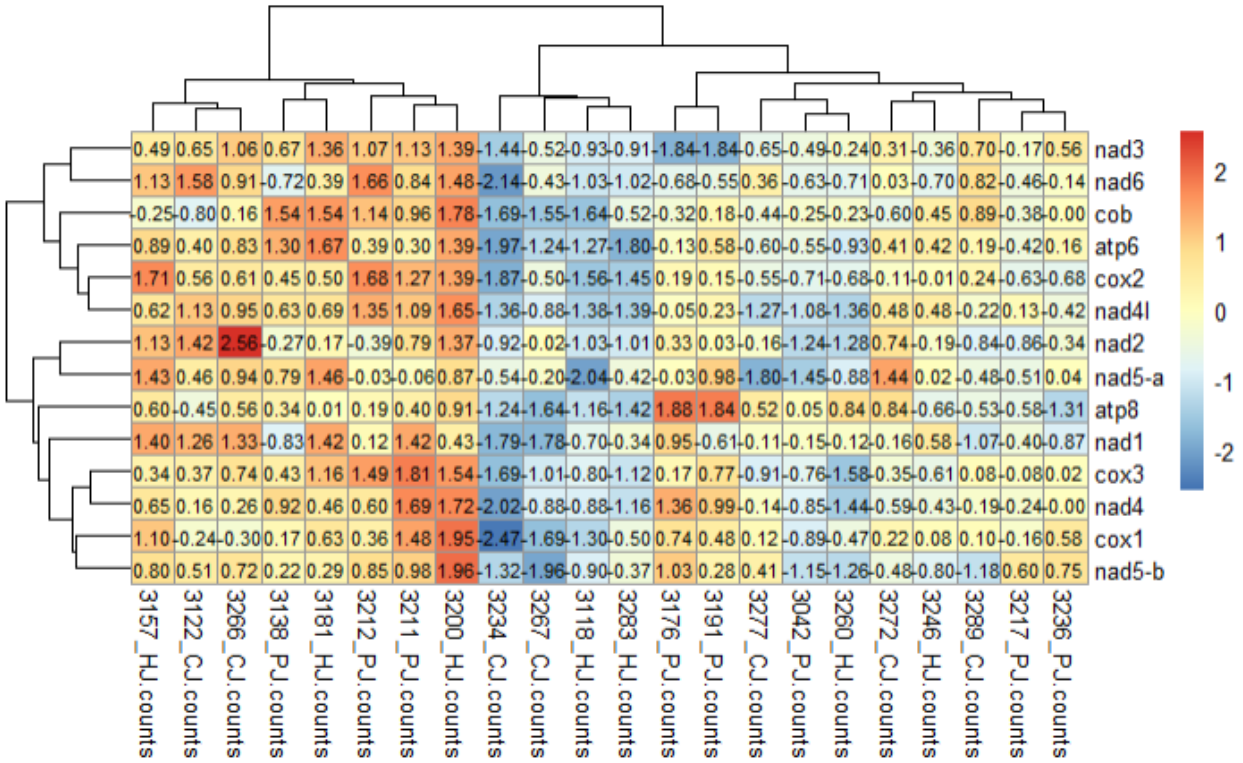

Figure 1: Heatmap of mitochondrially encoded genes from DEseq2 analysis. Heatmap shows Z-scores of the rlog transformed expression data from the DEseq dataset by gene. Hierarchical clustering is shown both by genet (PJ = palmata, CJ = cervicornis, HJ = hybrid) and by gene.

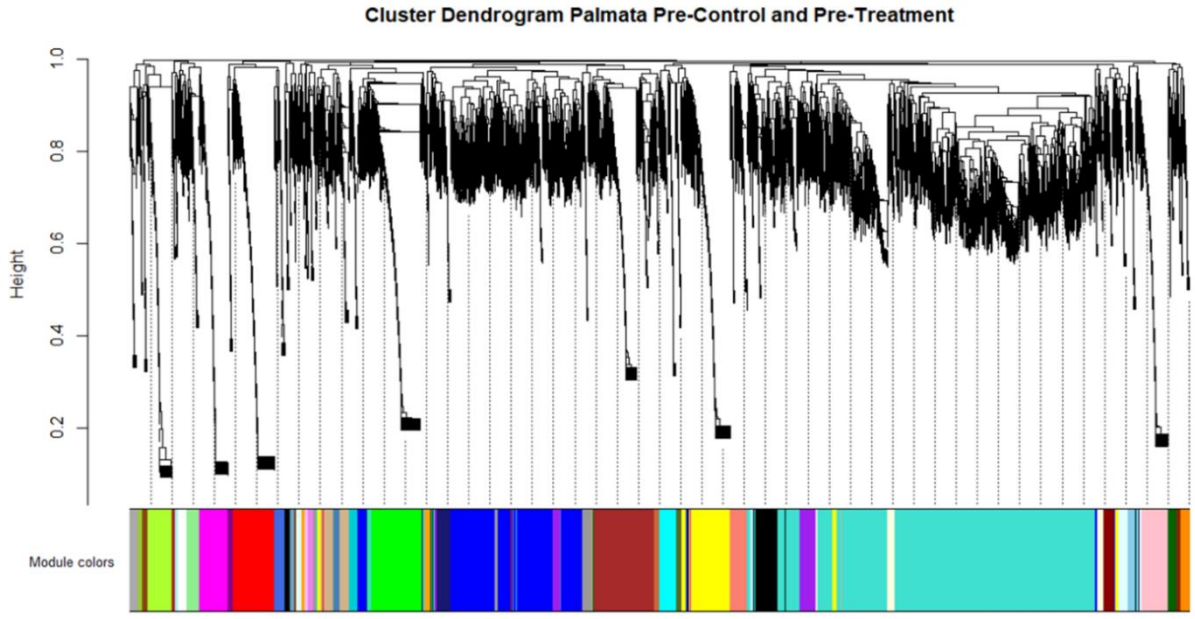

Figure 2: Clustering dendrogram of genes in the pre-control and pre-treatment *A. palmata* gene co-expression network (N = 7). Dissimilarity calculated using topological overlap measure (TOM). Module colors show the assigned module of each gene.

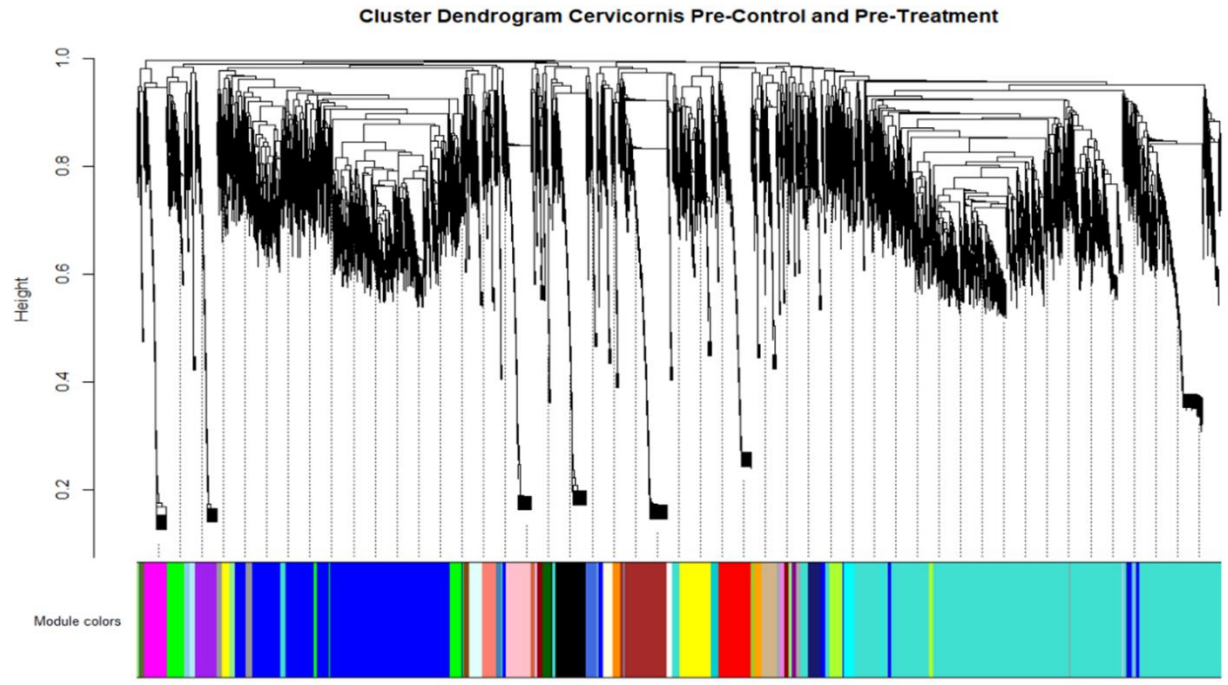

Figure 3: Clustering dendrogram of genes in the pre-control and pre-treatment *A. cervicornis* gene co-expression network (N = 7). Dissimilarity calculated using topological overlap measure (TOM). Module colors show the assigned module of each gene.

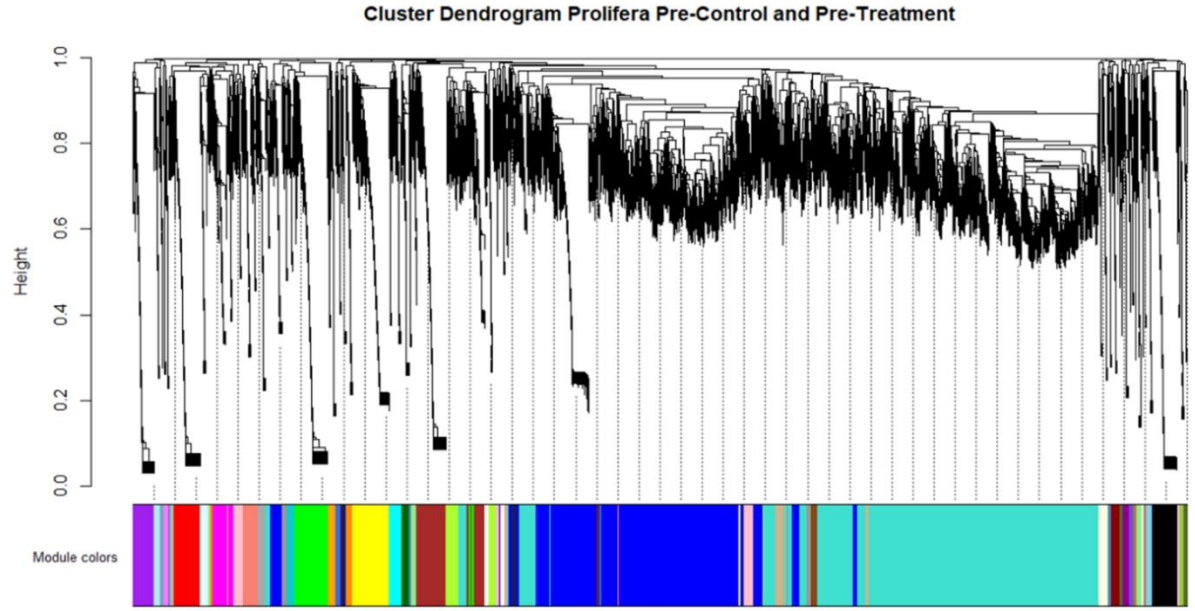

Figure 4: Clustering dendrogram of genes in the pre-control and pre-treatment *"A. prolifera"* gene co-expression network (N = 7). Dissimilarity calculated using topological overlap measure (TOM). Module colors show the assigned module of each gene

The mtDNA centric network for *A. palmata* built using topological overlap measure (TOM) with a threshold TOM > 0.02 had Mt-nad6 notably missing and forms two distinct connected components, suggesting that this taxon had the least amount of co-expression between its mtDNA genes when compared to other taxa (Figure 5). The mtDNA centric network for *A. cervicornis* had Mt-cob notably missing, had more edges than the *A. palmata* network, and forms only one connected component; this is clearly different from *A. palmata* network, indicating a greater degree of interconnectedness for *A. cervicornis* in terms of the co-expression of mtDNA genes (Figure 6). These results imply that co-expression is distinctly different between the parents. While missing Mt-atp8 from the network, the mtDNA centric network for *"A. prolifera"* features both the greatest number of edges and the greatest amount of interconnectedness among mtDNA genes (Figure 7). All of these networks were built using the TOM values reported in Tables 2-4 using a TOM >0.02 threshold. To test the effect of the threshold, it was decreased to TOM > 0.01 and the *A. palmata* mtDNA centric network was redone; this did have an effect as the missing Mt-nad6 was present and 6 more weak edges were added (TOM 0.011-0.016), with only 2 edges serving to bridge the connection between the two previously disconnected components (Figure 8).

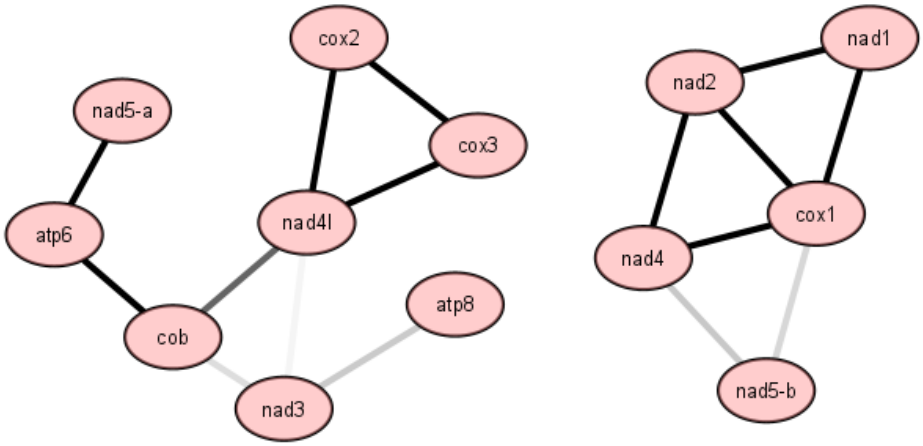

Figure 5: *A. palmata* mtDNA network (N = 13, E = 16), with edges showing topological overlap measure between mtDNA genes (TOM > 0.02), with color gradient showing TOM range of 0.020-0.261.

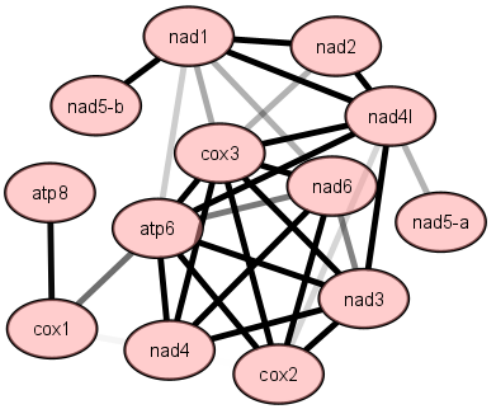

Figure 6: *A. cervicornis* mtDNA network (N = 13, E = 31), with edges showing TOM between mtDNA genes (TOM > 0.02), with color gradient showing TOM range of 0.025-0.219.

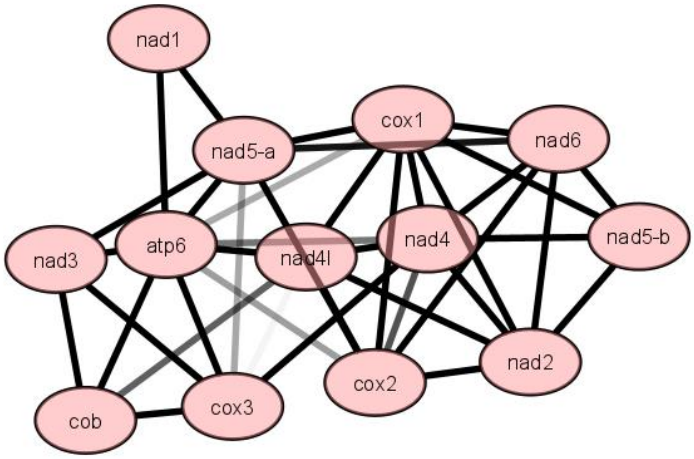

Figure 7: *"A. prolifera"* mtDNA network (N = 13, E = 39) with edges showing TOM between mtDNA genes (TOM > 0.02), with color gradient showing TOM range of 0.020-0.141.

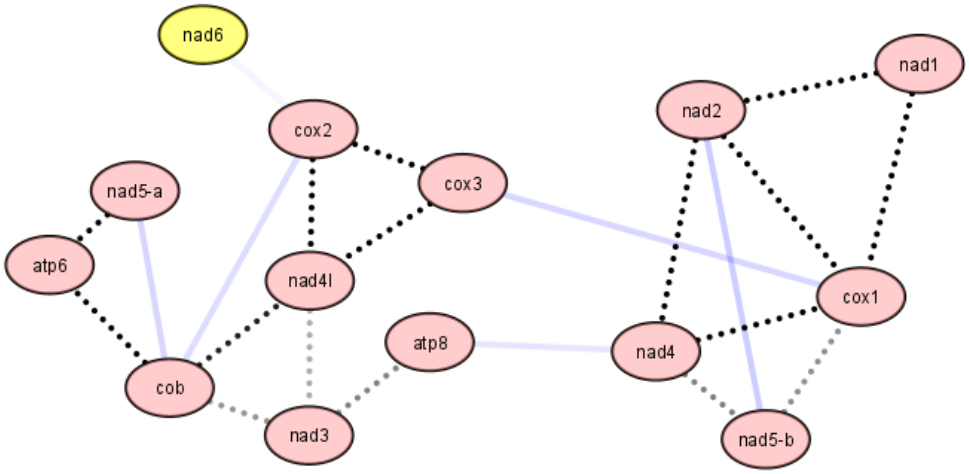

Figure 8: *A. palmata* mtDNA network (N = 14, E = 22) with edges showing TOM between mtDNA genes with decreased threshold (TOM > 0.01), with color gradient showing TOM range 0.011-0.261. Dotted edges were present when TOM threshold was 0.02, and solid blue edges were observed after the threshold decrease (TOM range 0.011-0.016). Nodes in yellow were seen after decreasing the threshold.

Table 22: Table showing edge weights (TOM) for *A. cervicornis* between mtDNA genes.

fromNode	toNode	weight
nad5-a	nad4l	0.031
nad1	nad2	0.081
nad1	nad6	0.031
nad1	atp6	0.028
nad1	cox3	0.032
nad1	nad4l	0.056
nad1	nad5-b	0.137
nad2	cox3	0.032
nad2	nad4l	0.054
nad6	atp6	0.037
nad6	nad4	0.137
nad6	cox3	0.055
nad6	cox2	0.074
nad6	nad3	0.036
atp6	nad4	0.067
atp6	cox3	0.086
atp6	cox2	0.059
atp6	nad4l	0.057
atp6	nad3	0.113
atp6	cox1	0.038
nad4	cox3	0.066
nad4	cox2	0.220
nad4	nad3	0.052
nad4	cox1	0.025
cox3	cox2	0.116
cox3	nad4l	0.073
cox3	nad3	0.169
cox2	nad4l	0.028
cox2	nad3	0.116
nad4l	nad3	0.058
atp8	cox1	0.048

Table 33: Table showing edge weights (TOM) for *A. palmata* between mtDNA genes.

fromNode	toNode	weight
nad5-a	atp6	0.093
nad1	nad2	0.050
nad1	cox1	0.061

cob	atp6	0.261
cob	nad4l	0.038
cob	nad3	0.023
nad2	nad4	0.123
nad2	cox1	0.151
nad4	nad5-b	0.026
nad4	cox1	0.128
cox3	cox2	0.077
cox3	nad4l	0.056
cox2	nad4l	0.099
nad4l	nad3	0.020
nad3	atp8	0.026
nad5-b	cox1	0.024

Table 44: Table showing edge weights (TOM) for *"A. prolifera"* between mtDNA genes

fromNode	toNode	weight
nad5-a	nad1	0.056
nad5-a	nad6	0.034
nad5-a	atp6	0.054
nad5-a	cox3	0.025
nad5-a	cox2	0.061
nad5-a	nad3	0.037
nad5-a	cox1	0.063
nad1	atp6	0.066
cob	atp6	0.051
cob	cox3	0.036
cob	nad4l	0.029
cob	nad3	0.057
nad2	nad6	0.141
nad2	nad4	0.098
nad2	cox2	0.108
nad2	nad4l	0.059
nad2	nad5-b	0.038
nad2	cox1	0.068
nad6	nad4	0.099
nad6	cox2	0.072
nad6	nad5-b	0.051
nad6	cox1	0.085
atp6	nad4	0.028
atp6	cox3	0.060
atp6	cox2	0.025

atp6	nad4l	0.072
atp6	nad3	0.068
atp6	cox1	0.025
nad4	cox3	0.049
nad4	cox2	0.030
nad4	nad4l	0.086
nad4	nad5-b	0.087
nad4	cox1	0.083
cox3	nad4l	0.020
cox3	nad3	0.106
cox2	nad4l	0.056
cox2	cox1	0.088
nad4l	cox1	0.098
nad5-b	cox1	0.054

After clustering analysis, modules containing the mtDNA were identified and differences in module membership among taxa were recorded. For this analysis, mtDNA genes either 1) clustered with the same pattern across all three taxa, 2) clustered with a different pattern across all three taxa, or 3) clustered similarly only between the parental taxa when compared to the hybrid. The mtDNA gene atp8 and Nad5-b clustered similarly among all three taxa because each of them clustered without any of the other mitochondrially encoded genes. However, top 10 hub genes based on ranked module membership were compared among taxa for each of these modules and there was no overlap (supplemental tables 1-6). The mtDNA gene Nad5-a clustered similarly between the parents and differently in the hybrid. In *A. palmata* and *A. cervicornis*, it clustered without any other mitochondrially encoded genes. In *"A. prolifera"*, it clustered in a

module with both cox1 and cox2. All of the other mtDNA genes showed completely different patterns of regulation among all three taxa.

Chapter 4

Discussion

This experiment investigated whether hybrid breakdown in the F2 generation of coral hybrids in Caribbean acroporid corals could be attributed to mitonuclear conflict. The large variation in expression among genets overrode clear signals of taxon-specific expression of mitochondrial genes. The lack of co-expression of mitochondrial genes indicated that there could be technical errors in the data analysis that should be investigated. Also, light stress due to failed acclimation of *A. palmata* to its new common garden environment when compared to the other taxa should be investigated to determine if this could explain the observed breakdown in its mtDNA network. Thus, the question as to whether mitonuclear conflict could be effecting these hybrids is still unclear, prompting the need for future investigations into this topic.

More specifically, the wide variation of expression between genets and the lack of clustering by taxon in the differential expression analysis suggest that downstream network analyses would be difficult to use for finding differences in the co-expression of mtDNA genes by taxon (Figure 1). *A. palmata* and *"A. prolifera"* co-expression both have a total of 39 modules while *A. cervicornis* has 38 modules, suggesting through module preservation that the hybrid is more similar to *A. palmata* (figures 2-4), though marginally so at least for this metric. Analysis of mtDNA centric networks shows large differences in the number of edges between *A. palmata* and *A. cervicornis*, suggesting further difference between the parents when looking at

mtDNA co-expression (figure 5-6). Presumably, each of these parental species should feature a functional oxidative phosphorylation pathway without significant variation since even slight variation can lead to altered ATP production in the mitochondria (Hill, 2015), making the above findings quite surprising. Analysis of the mtDNA centric network for *"A. prolifera"* shows the highest degree of co-expression between mtDNA genes as seen by the large number of edges in the network in comparison to the parental taxa (figure 5-8). This finding suggests the hybrid may have co-expression patterns more similar to *A. cervicornis* since the co-expression of mtDNA of *A. palmata* appears to be disrupted regardless of TOM threshold (Figure 8); however, this is contradictory to the findings of the module numbers above, which instead saw more similarity between the hybrid and *A. palmata.*

It was also found that all the mtDNA genes clustered separately among many different modules, suggesting that these mtDNA genes are not being co-expressed similarly when comparing the three taxa. In addition, relatively low topological overlap measure values across all of the constructed mtDNA centric networks suggest that these mtDNA genes are not strongly interconnected (Tables 2-4). All three networks were missing one mtDNA protein encoded gene, though the specific gene was different between the three taxa. This indicates that these three particular mtDNA genes were not strongly connected with any of the other mtDNA genes as determined by the TOM > 0.02 cutoff. Even when the TOM cutoff was decreased to 0.01, *A. palmata* had a lower number of edges and thus is shown to have low interconnection in terms of mtDNA co-expression (Figure 8). This is contradictory to other studies that find that all mtDNA genes are strongly interconnected using a higher TOM threshold (Yuan et al., 2020; Ojala et al., 1981). As such, we would expect mtDNA genes involved in OXPHOS to cluster together since they should be highly co-expression and thus strongly interconnected. Since this is not the case

in these Acroporid networks (Figure 5-7), this suggests that the clustering method used in my analysis was not ideal. This makes the relationship between parental gene expression and the hybrids unclear and prompts the need to examine sources of error.

To start, improvement of the clustering method using an additional k-means clustering step reportedly improves the clustering method (Hou et al., 2021). Another possible source of error could have occurred upstream of the network assembly when the secondary alignment step was carried out for the mitochondrial gene counts. STAR has been shown to have higher numbers for gene counts when compared to Kalisto and Bowtie2 (Du et al., 2020). However, Kalisto needed to align TAGseq reads to the mitochondrial genome. Future works should look at comparing alignment quality with each tool in order to verify that these patterns of low interconnectedness hold true, regardless of the aligner tool chosen.

Lastly, the site where the common garden was set up was at a depth favoring *A. cervicornis* over the other taxa, which may explain its superior physiological performance in comparison to the other two taxa after exposure to heat stress (Osborne, C. C., et al., in prep). Typically, *A. cervicornis* is found at deeper depths of up to 20 meters while *A. palmata* prefers shallower depths of less than 10 meters (Adey & Burke, 1976; Fenner, 1988). These depths were slightly different in this region in Belize with natal depths varying from 0.7m to 14m, with *A. cervicornis* occupying the deepest depths (Osborne, C. C., et al., in prep). However, in this experiment, all coral species were taken from their native environments and acclimated to a new common garden environment with the same depth of ~4 meters (Osborne, C. C., et al., in prep). Since corals are sensitive to changes in light (Durante et al., 2019), the *A. palmata* samples may have been stressed due to their movement into a novel light environment found in the common garden environment; *A. palmata* likely did not fully acclimate to this new environment when

compared to *A. cervicornis* and *"A. prolifera"*. Further evidence of this stress for *A. palmata* is shown as *A. palmata* had the strongest and most detrimental physiological response to heat stress. This may suggest that even under control conditions, *A. palmata* experienced environmental stress when compared to the other taxa due to the depth it was placed, meaning that it may have experienced differences in gene expression as a result (Osborne, et al., in prep). These differences in expression could have extended to the critical mtDNA genes this project analyzed, which would have disrupted the co-expression of these genes and thus altered the mtDNA gene co-expression network (Figures 5-8). Though not analyzed for this honors thesis project, samples were collected from the natal reef environment in Belize for the three taxa and exposed to the same heat stress experiment as the common garden samples. In this experiment, the performance of the two parents flipped, with *A. palmata* performing better than *A. cervicornis* after heat exposure, and the hybrid showing signs of hybrid vigor (Osborne C. C., et al., in prep). To verify that *A. palmata* mtDNA co-expression network features less connectivity compared to the other taxa, this analysis should be carried out on the natal-depth derived samples.

Overall, it cannot be determined based on these findings whether hybridization in acroporid corals results in mitonuclear conflict that could lead to F2 hybrid breakdown. We found that in all three taxa, the co-expression between mtDNA genes was relatively low compared to other studies based on topological overlap measure (Yuan et al., 2020; Ojala et al., 1981). This would suggest that the parents along with the hybrid would struggle to survive since the breakdown of co-expression among mtDNA leads to potentially fatal mitonuclear conflict due to reduced efficiency of ATP production (Hill, 2016; Burton et al., 2006). Since this is obviously not the case as the parents and F1 hybrid do survive for hundreds to even thousands of

years, upstream parameters should be checked and tweaked, and the natal depth samples should be incorporated for comparison. If *A. palmata* continues to show a large breakdown in mtDNA co-expression when compared the other taxa after these alterations are made, it could be concluded that *A. palmata* has intrinsically disrupted mtDNA expression that is not influenced by factors like light stress as a result of failed common garden acclimation. If a breakdown in mtDNA co-expression is detected specifically for the hybrid when compared to the parental taxa after these changes are implemented, it could be concluded that mitonuclear conflict may result from this hybridization event. However, if there is no distinct breakdown in the co-expression of mtDNA genes for the hybrid when compared to the parents, this would suggest that mitonuclear conflict should not be considered as a factor contributing to F2 hybrid breakdown in acroporid corals.

Appendix A

Supplemental Information, Figures, and Tables

WGCNA:

WGCNA involves using similarity and adjacency measures to construct the network as well as hierarchical clustering and a program called Dynamic tree cut to detect modules (Langfelder & Hovarth, 2008). The nodes of each network are genes, which each has a defined expression profile x_i. WGCNA begins with network construction and defining co-expression similarity measure s_{ij} to described the similarity between genes i and j as the correlation between the RNAseq expression profiles of each gene: $s_{ij}^{unsigned}$ = |cor(x_i , x_j)| (Langfelder & Hovarth, 2008). In this analyses, a signed network was built in order assess positive and negative correlations between the pairwise expression profiles of all genes in the network. A signed network is most appropriate for in order to find modules that are biologically meaningful (Mason et al., 2009). Thus, the following equation was used to define the co-expression similarity measure: $s_{ij}^{signed} = |0.5 + 0.5cor(x_i , x_j)|$. This Pearson correlation, which did range from -1 (anticorrelated) to 1 (perfectly correlated), is transformed to range from 0 (anticorrelated) to 1 (perfectly correlated). This could be used to build a similarity matrix, resulting in an undirected weighted network in which every pair of nodes with a non-zero correlation has a weighted edge. This network would be too dense, prompting the need for a threshold to be imposed to reduce the number of edges. This is done by imposing soft-thresholding parameters to define the weighted network adjacency a_{ij}, which is used to build an adjacency matrix A to show how strongly genes are connected. Thus, the weighted network adjacency is calculated by raising the co-expression

similar s_{ij} to a power $\beta \geq 1$ using soft- thresholding parameters: $a_{ij} = (s_{ij})^{\beta}$ (Langfelder & Hovarth, 2008). The higher the power β, the more emphasis is placed on correlations that are higher (and thus the less influence is placed on correlations that are lower). Choice of soft thresholding power for each network was done following scale free topology criterion in order to ensure the degree distribution of the network follows a power law, with many genes having low number of connections and few "hub" genes having a high connectivity. This choice was done following the tutorial by Langfelder and Hovarth and involves picking the lowest power with a reasonable scale free topology model fit index and a low mean connectivity value (Supplemental figures 1-3).

After weighted network adjacency is defined for each mitonuclear co-expression network, modules are detected for each network using hierarchical clustering and Dynamic Branch Cut methods (Langfelder & Hovarth, 2008). Modules themselves are just clusters of interconnected genes based on a measure of network proximity. A proximity of 1 is the maximum interconnectedness between two genes while a proximity of 0 is the minimum interconnected measure between two gene. More specifically, proximity in WGCNA is measured using a topological overlap measure (TOM). This measure considered both the adjacency a_{ij} between the two genes in question as well as connectivity between neighbors that they have in common, resulting in a more robust proximity measure (Langfelder & Hovarth, 2008). Proximity measures are than fed into average linkage hierarchical clustering to create a dendrogram (Langfelder & Hovarth, 2008). Then, each branch of the dendrogram that is considered a module can be found using Dynamic Branch cut methods (Langfelder & Hovarth, 2008).

Supplemental Figures:

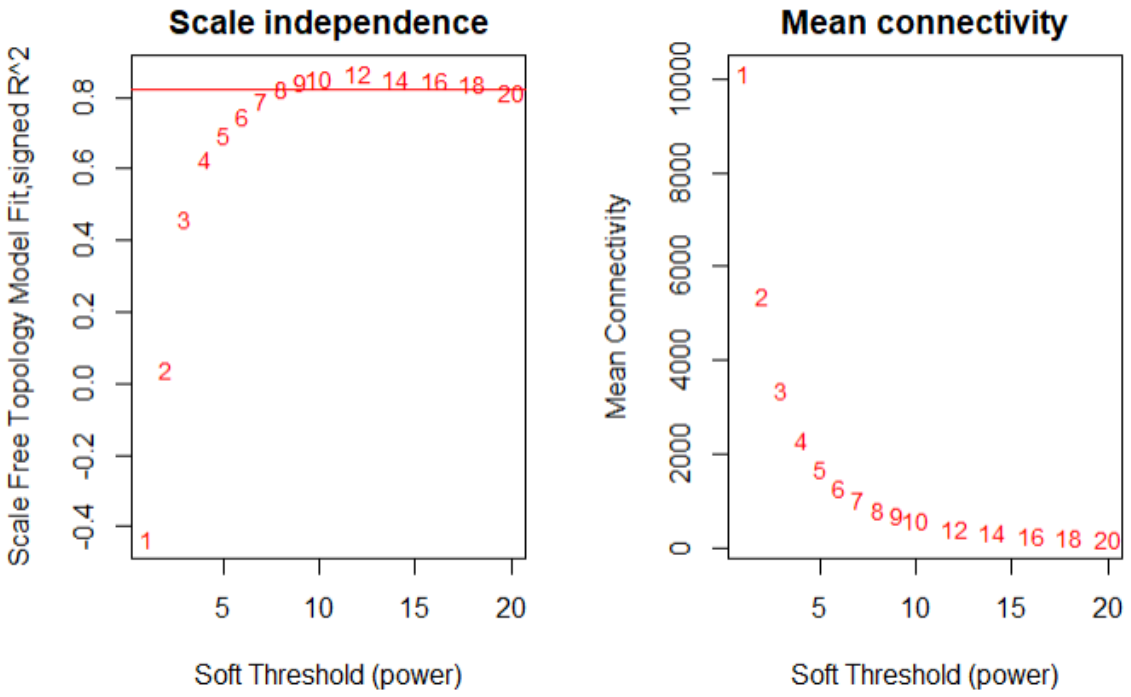

Supplemental Figure 1: Pre-control and pre-treatment *A. palmata* (N = 7) network topology analysis performed with soft- thresholding powers. The left graph shows scale free topology model fit index as a function of the soft thresholding power. The right graph shows mean connectivity as a function of the soft thresholding power. An ideal soft-thresholding power would be the lowest power with a scale free topology model fit index (R^2) that is greater than 0.9. Subsequent larger powers would form an asymptote and appear to reach a limit at around 0.9. However, based on the plot, none of the R^2 values are greater than 0.9, but they appear to form an asymptote around 0.82, which is approximately 0.9. 16 was thus chosen both for its higher R^2 value (~0.88) and low mean connectivity (~258.56). Choice of 16 as the power would allow the constructed network to follow approximate scale free topology.

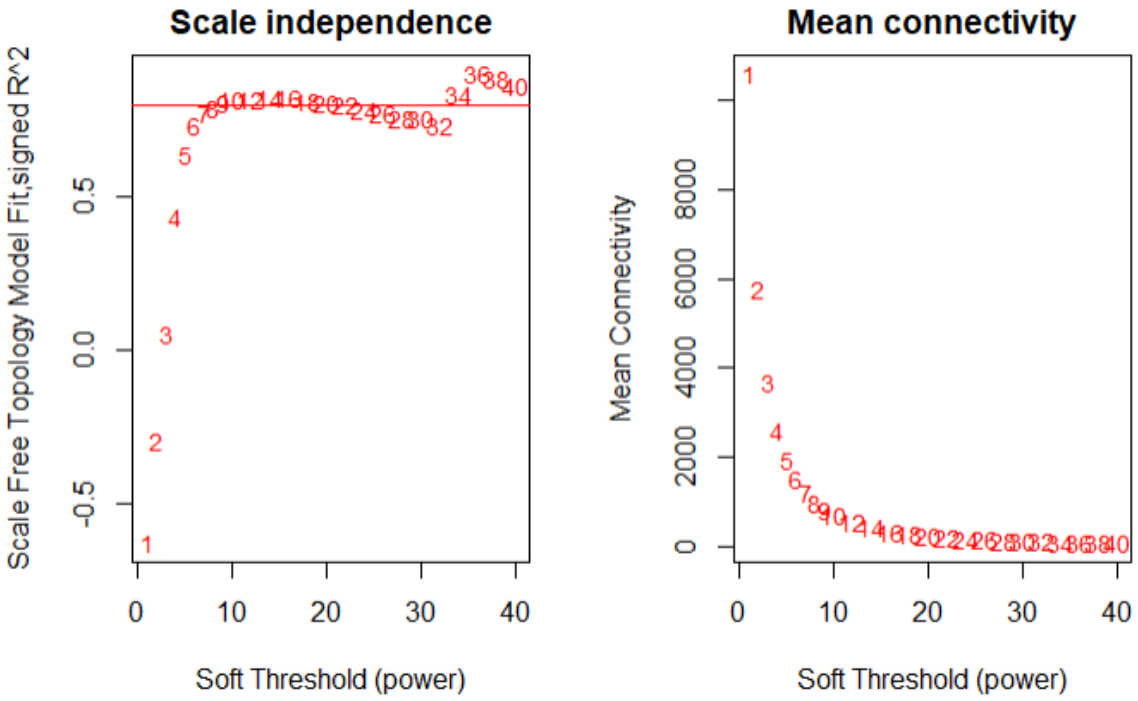

Supplemental Figure 2: Pre-control and pre-treatment *A. cervicornis* (N = 7) network topology analysis performed with soft- thresholding powers. Based on the plot, none of the R^2 values are greater than 0.9, but they appear to form an asymptote around 0.8, which is approximately 0.9. 14 was thus chosen both for its higher R^2 value (~0.825) and low mean connectivity (~430.89). Choice of 14 as the power would allow the constructed network to follow approximate scale free topology.

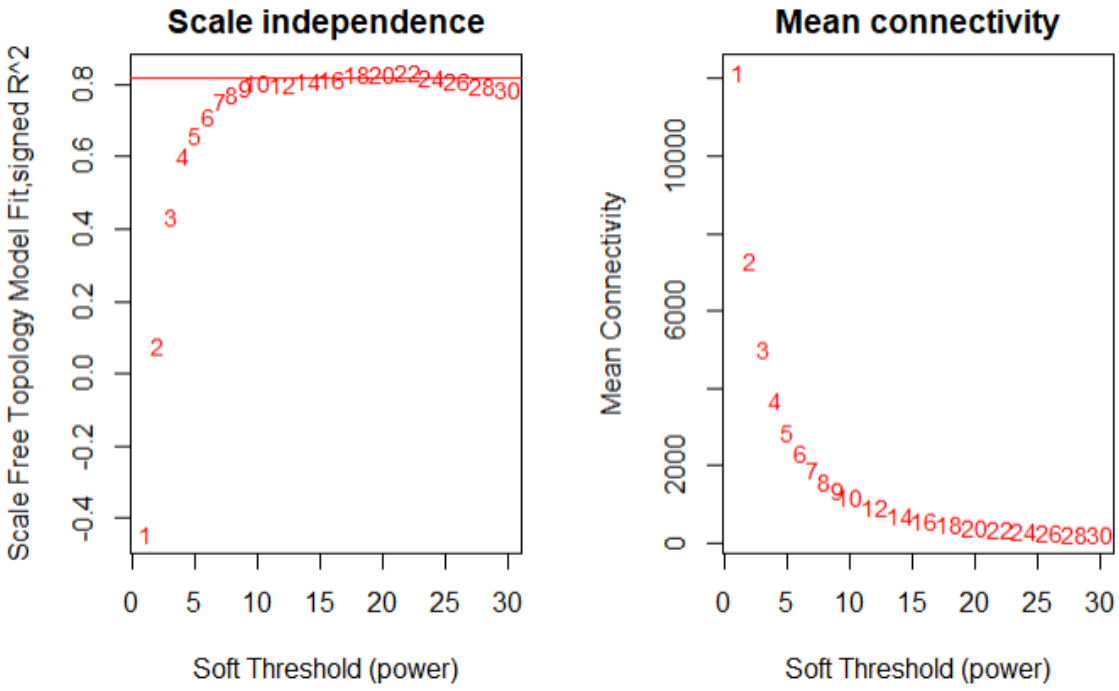

Supplemental Figure 3: Pre-control and pre-treatment *"A. prolifera"* (N = 7) network topology analysis performed with soft- thresholding powers. Based on the plot, none of the R^2 values are greater than 0.9, but they appear to form an asymptote around 0.82, which is approximately 0.9. 22 was thus chosen both for its higher R^2 value (~0.833) and low mean connectivity (~380.45). Choice of 22 as the power would allow the constructed network to follow approximate scale free topology.

Supplemental Tables:

Supplemental Table 1: *A. palmata* ATP8 "cyan" Top 10 Hub Genes based on module membership (MM).

Hub Gene	Module Membership (MM)
Mitogen-activated protein kinase kinase kinase A	0.978
Plasmepsin V	0.969
Probable serine/threonine-protein kinase pats1,Probable serine/threonine-protein kinase pats1	0.968
Vitelline membrane outer layer protein 1	0.967
50S ribosomal subunit assembly factor BipA	0.966
A disintegrin and metalloproteinase with thrombospondin motifs 9	0.966
Aspartic proteinase-like protein 1	0.966

Cytochrome b561, DM13 and DOMON domain-containing protein At5g54830	0.966
Cytochrome P450 714B2	0.966
Cytohesin-4	0.966

Supplemental Table 2: *A. cervicornis* ATP8 "skyblue" Top 10 Hub Genes based on module membership (MM).

Hub Gene	Module Membership (MM)
40S ribosomal protein S15-B	0.990
85/88 kDa calcium-independent phospholipase A2	0.990
Beta-glucosidase 34	0.990
PREDICTED: uncharacterized protein LOC107332376	0.990
uncharacterized protein LOC111345499	0.990
PREDICTED: uncharacterized protein LOC107348504 isoform X1	0.983
Exonuclease 3'-5' domain-containing protein 1	0.979
Acid-sensing ion channel 1C	0.968
atp8	0.959
DNA double-strand break repair Rad50 ATPase	0.947

Supplemental Table 3: *"A. prolifera"* ATP8 "midnightblue" Top 10 Hub Genes based on module membership (MM).

Hub Gene	Module Membership (MM)
Centrosomal protein of 44 kDa	0.985
Proteasome subunit alpha type-1	0.971
E3 ubiquitin-protein ligase SIAH1A	0.97
Sphingosine 1-phosphate receptor 3	0.964
DNA-(apurinic or apyrimidinic site) lyase	0.957
Ocellar opsin	0.951
Citrate synthase-lysine N-methyltransferase CSKMT, mitochondrial	0.947
PREDICTED: uncharacterized protein LOC107344570	0.947
Protein FAM49B	0.947
UBX domain-containing protein 10	0.943

Supplemental Table 4: *A. palmata* Nad5-b "royalblue" Top 10 Hub Genes based on module membership (MM).

Hub Gene	Module Membership (MM)
WD repeat-containing protein 26	0.976
GRB2-associated-binding protein 2	0.966
PREDICTED: uncharacterized protein LOC107336505 isoform X2	0.956
Feruloyl esterase B	0.955
1,4-alpha-glucan-branching enzyme 2-1, chloroplastic/amyloplastic	0.932
Ankyrin repeat domain-containing protein 1	0.932
Calcium/calmodulin-dependent protein kinase type II delta 1 chain	0.932
Ferric reduction oxidase 6	0.932
Formin-like protein 8	0.932
hypothetical protein AWC38_SpisGene8964	0.932

Supplemental Table 5: *A. cervicornis* Nad5-b "lightgreen" Top 10 Hub Genes based on module membership (MM).

Hub Gene	Module Membership (MM)
Ras-related protein Rab-30	0.991
PREDICTED: uncharacterized protein LOC107332373 isoform X1	0.978
Tetratricopeptide repeat protein 36 homolog	0.973
60S ribosomal protein L18-2	0.964
Ubiquitin carboxyl-terminal hydrolase MINDY-1	0.946
Calcium/calmodulin-dependent 3',5'-cyclic nucleotide phosphodiesterase 1B	0.946
PREDICTED: uncharacterized protein LOC107328003	0.942
Cyclin-dependent kinase-like 2	0.938
Sorting nexin-8,Sorting nexin-8	0.937
PAX-interacting protein 1	0.932

Supplemental Table 6: *"A. prolifera"* Nad5-b "blue" Top 10 Hub Genes based on module membership (MM).

Hub Gene	Module Membership (MM)
Sulfate/thiosulfate import ATP-binding protein CysA	0.999
Putative quercetin 2,3-dioxygenase PA1210	0.998
2,3-bisphosphoglycerate-dependent phosphoglycerate mutase	0.997
S-adenosylmethionine synthase 3	0.997

Putative transcription elongation factor SPT5 homolog 1	0.997
Peptidyl-prolyl cis-trans isomerase CYP22	0.997
Chlorophyll a-b binding protein LI818, chloroplastic	0.997
Formin-1	0.996
Cytochrome c6	0.996
Adenylate kinase 7	0.994

References

Adey, W. H., & Burke, R. (1976). Holocene bioherms (algal ridges and bank-barrier reefs) of the eastern caribbean. *Geological Society of America Bulletin*, 87(1), 95-109. https://doi.org/10.1130/0016-7606(1976)87<95:HBARAB>2.0.CO;2

Bray, N. L., Pimentel, H., Melsted, P., & Pachter, L. (2016). Near-optimal probabilistic RNA-seq quantification. *Nature Biotechnology*, 34(5), 525-527. https://doi.org/10.1038/nbt.3519

Burton, R. S., Ellison, C. K., & Harrison, J. S. (2006). The sorry state of F2 hybrids: Consequences of rapid mitochondrial DNA evolution in allopatric populations. *The American Naturalist*, 168(S6), S14-S24. https://doi.org/10.1086/509046

Burton, R. S., Pereira, R. J., & Barreto, F. S. (2013). Cytonuclear genomic interactions and hybrid breakdown. *Annual Review of Ecology, Evolution, and Systematics*, *44*(1), 281-302. https://doi.org/10.1146/annurev-ecolsys-110512-135758

Chou, J., & Leu, J. (2015). The red queen in mitochondria: Cyto-nuclear co-evolution, hybrid breakdown and human disease. *Frontiers in Genetics*, *6*, 187-187. https://doi.org/10.3389/fgene.2015.00187

Ding, Y., Chen, W., Li, Q., Rossiter, S. J., & Mao, X. (2021). Mitonuclear mismatch alters nuclear gene expression in naturally introgressed rhinolophus bats. Frontiers in Zoology, 18(1), 42-42. https://doi.org/10.1186/s12983-021-00424-x

Du, Y., Huang, Q., Arisdakessian, C., & Garmire, L. X. (2020). Evaluation of STAR and kallisto on single cell RNA-seq data alignment. *G3 : Genes - Genomes - Genetics*, *10*(5), 1775-1783. https://doi.org/10.1534/g3.120.401160

Durante, M. K., Baums, I. B., Williams, D. E., Vohsen, S., & Kemp, D. W. (2019). What drives phenotypic divergence among coral clonemates of *Acropora palmata*? Molecular Ecology, 28(13), 3208-3224. https://doi.org/10.1111/mec.15140

Ellison, C. K., & Burton, R. S. (2010). Cytonuclear conflict in interpopulation hybrids: The role of RNA polymerase in mtDNA transcription and replication. *Journal of Evolutionary Biology*, *23*(3), 528-538. https://doi.org/10.1111/j.1420-9101.2009.01917.x

Fenner, D. P. (1988). Some leeward reefs and corals of cozumel, mexico. *Bulletin of Marine Science*, 42(1), 133-144.

Fogarty ND (2010) Reproductive isolation and hybridization dynamics in threatened Caribbean acroporid corals. PhD dissertation, Florida State University, Tallahassee

Fogarty, N. D. (2012;2011;). Caribbean acroporid coral hybrids are viable across life history stages. Marine Ecology. Progress Series (Halstenbek), 446, 145-159. https://doi.org/10.3354/meps09469

Hill, G. E. (2015). Mitonuclear ecology. *Molecular Biology and Evolution, 32*(8), 1917-1927. https://doi.org/10.1093/molbev/msv104

Hill, G. E. (2016). Mitonuclear coevolution as the genesis of speciation and the mitochondrial DNA barcode gap. *Ecology and Evolution, 6*(16), 5831-5842. https://doi.org/10.1002/ece3.2338

Hill, G. E. (2017). The mitonuclear compatibility species concept. The Auk, 134(2), 393-409. https://doi.org/10.1642/AUK-16-201.1

Hou, J., Ye, X., Li, C., & Wang, Y. (2021). K-module algorithm: An additional step to improve the clustering results of WGCNA co-expression networks. *Genes*, 12(1), 87. https://doi.org/10.3390/genes12010087

Japaud, A., Fauvelot, C., & Bouchon, C. (2014). Unexpected high densities of the hybrid coral acropora prolifera (lamarck 1816) in guadeloupe island, lesser antilles. *Coral Reefs*, 33(3), 593-593. https://doi.org/10.1007/s00338-014-1169-7

Keck, J., Houston, R. S., Purkis, S., & Riegl, B. M. (2005). Unexpectedly high cover of acropora cervicornis on offshore reefs in roatán (honduras). Coral Reefs, 24(3), 509-509. https://doi.org/10.1007/s00338-005-0502-6

Kitchen, S. A., Osborne, C. C., Fogarty, N. D., Baums, I. B. (2021). Morphotype is not linked to mitochondrial haplogroups of Caribbean acroporid hybrids.

Lane, N. (2011). Mitonuclear match: Optimizing fitness and fertility over generations drives ageing within generations: Problems and paradigms. *Bioessays, 33*(11), 860-869.

Langfelder, P., & Horvath, S. (2008). WGCNA: An R package for weighted correlation network analysis. *BMC Bioinformatics*, 9(1), 559-559. https://doi.org/10.1186/1471-2105-9-559

Lee-Yaw, J. A., Jacobs, C. G. C., & Irwin, D. E. (2014). Individual performance in relation to cytonuclear discordance in a northern contact zone between long-toed salamander (ambystoma macrodactylum) lineages. *Molecular Ecology, 23*(18), 4590-4602. https://doi.org/10.1111/mec.12878

Love, M. I., Huber, W., & Anders, S. (2014). Moderated estimation of fold change and dispersion for RNA-seq data with DESeq2. Genome Biology (Online Edition), 15(12), 550-550. https://doi.org/10.1186/s13059-014-0550-8

Mason, M. J., Fan, G., Plath, K., Zhou, Q., & Horvath, S. (2009). Signed weighted gene co-expression network analysis of transcriptional regulation in murine embryonic stem cells. *BMC Genomics, 10*(1), 327-327. https://doi.org/10.1186/1471-2164-10-327

van Oppen, Madeleine J. H, Willis, B. L., Van Rheede, T., & Miller, D. J. (2002). Spawning times, reproductive compatibilities and genetic structuring in the acropora aspera group: Evidence for natural hybridization and semi-permeable species boundaries in corals. *Molecular Ecology, 11*(8), 1363-1376. https://doi.org/10.1046/j.1365-294X.2002.01527.x

Ojala, D., Montoya, J., & Attardi, G. (1981). tRNA punctuation model of RNA processing in

human mitochondria. *Nature (London)*, *290*(5806), 470-474. https://doi.org/10.1038/290470a0

Oppen, M. J. H. Van, Willis, B. L., Vugt, H. W. J. A. Van, & Miller, D. J. (2000). Examination of species boundaries in the acropora cervicornis group (scleractinia, cnidaria) using nuclear DNA sequence analyses. *Molecular Ecology*, *9*(9), 1363-1373. https://doi.org/10.1046/j.1365-294x.2000.01010.x

Osborne, C. C, … Fogarty, N., Baums, I, B. (in prep). Heterosis in an F1 Coral Hybrid; Implications for Restoration in a Warming Ocean.

Rank, N. E., Mardulyn, P., Heidl, S. J., Roberts, K. T., Zavala, N. A., Smiley, J. T., & Dahlhoff, E. P. (2020). Mitonuclear mismatch alters performance and reproductive success in naturally introgressed populations of a montane leaf beetle. *Evolution*, *74*(8), 1724-1740. https://doi.org/10.1111/evo.13962

Richards, Z. T., & Hobbs, J. A. (2015). Hybridisation on coral reefs and the conservation of evolutionary novelty. Current Zoology, 61(1), 132-145. https://doi.org/10.1093/czoolo/61.1.132

Sagan, L. (1967). On the origin of mitosing cells. *Journal of Theoretical Biology*, *14*(3), 225,IN1-274,IN6. https://doi.org/10.1016/0022-5193(67)90079-3

Shannon, P., Markiel, A., Ozier, O., Baliga, N. S., Wang, J. T., Ramage, D., Amin, N., Schwikowski, B., & Ideker, T. (2003). Cytoscape: A software environment for integrated models of biomolecular interaction networks. Genome Research, 13(11), 2498-2504. https://doi.org/10.1101/gr.1239303

Vollmer, S. V., & Palumbi, S. R. (2002). Hybridization and the evolution of reef coral diversity. *Science (American Association for the Advancement of Science)*, *296*(5575), 2023-2025. https://doi.org/10.1126/science.1069524

Wallace, D. C. (2007). Why do we still have a maternally inherited mitochondrial DNA? insights from evolutionary medicine. *Annual Review of Biochemistry*, *76*(1), 781-821. https://doi.org/10.1146/annurev.biochem.76.081205.150955

Wang, G., Yang, E., Mandhan, I., Brinkmeyer-Langford, C. L., & Cai, J. J. (2014). Population- level expression variability of mitochondrial DNA-encoded genes in humans. *European Journal of Human Genetics* : EJHG, 22(9), 1093-1099. https://doi.org/10.1038/ejhg.2013.293

Wheaton, J., Beaver, C., Jaap, W., Callahan, M., Kupfner, S., Wade, S., Gilliam, D. S., Ettinger, B. D., Fahy D. P., Gill, S. M., Klink, L, H., Monty, J. A., Philips, M. A., Shuman, L. F., Stephens, N. R., Walker, B. K., Walczak, J. C., Dodge, R. E., McIntosh, T., Blair, S., Banks, K., Fisher L. E., Stout D., Ligas J., and Phipps J., (2006) Southeast Florida Coral Reef Evaluation and Monitoring Project 2005 Year 3 Final Report : 1 -25. https://nsuworks.nova.edu/occ_facreports/70

Yuan, Y., Ju, Y. S., Kim, Y., Li, J., Wang, Y., Yoon, C. J., Yang, Y., Martincorena,

I., Creighton, C. J., Weinstein, J. N., Xu, Y., Han, L., Kim, H., Nakagawa, H., Park, K., Campbell, P. J., Liang, H., & PCAWG Consortium. (2020). Comprehensive molecular characterization of mitochondrial genomes in human cancers. Nature Genetics, 52(3), 342-352. https://doi.org/10.1038/s41588-019-0557-x

ACADEMIC VITA

Bryan Manzano

Skills Summary

Research

Learned basic skills in RNA extraction from coral tissue, bioinformatic analysis using various coding languages, and WGCNA analysis to use in coral hybridization research advised by Dr. Illiana Baums. Additional experience with serial dilution, gel electrophoresis, PCR, and data analysis gained from the Freshman Research Initiative at Penn State.

Teaching

Responsible for teaching a lab section as a Teaching Assistant for an Ecology and Evolution class led by Dr. Carla Hass. Additional experience as university learning assistant for introductory chemistry.

Programming

Basic knowledge of R, command line, and MATLAB from lab thesis research, summer internship, and bioinformatics class.

Education

The Pennsylvania State University | University Park, PA 16802

- Bachelor of Science: Biology, General Option and Bachelor of Musical Arts: French horn performance
- Schreyer Honors College
- Graduation: May 2023
- Dean's List (7 semesters)
- Student Marshal 2023 Eberly College of Science
- Student Marshal 2023 College of Arts and Architecture

Research Experience

Baums Coral Lab | 2020-current

Honors thesis research is being supervised by Dr. Illiana Baums. Wrote a literature review paper discussing the effects of mitonuclear conflict on F2 hybrid breakdown of *Acropora prolifera*

with guidance from Professor Baums and graduate students. Interned for the Baums lab as a Research Assistant in summer of 2022 in order to learn RNA extraction protocol from tissues of various species of coral, and continuing internship to improve RNA extraction protocol for the spring 2023 semester. Currently continuing to work on developing original code for honors thesis research that uses a network approach via differential gene expression analyses and WGCNA to compare individually constructed networks for a coral hybrid (*Acropora prolifera*) and its two parental species to look for evidence of disrupted co-expression between mitochondrial genes and nuclear genes that code for mitochondrial proteins. If evidence of topological change in critical parts of these mitonuclear networks is found for the hybrid when compared to parental taxa, it could show evidence for mitonuclear conflict due to the hybridization that could have downstream effects that impact hybrid performance and subsequent future hybrid offspring production.

Freshman Research Initiative | 2019-2020

Learned basics of the scientific method, serial dilution, gel electrophoresis, and PCR in preparation for carrying out an original research project. The research project involved working with Dr. Hidetoshi Inamine and Dr. Kim Nelson with plans to perform an original experiment on the effects of Frequency and Intensity of Disturbance on *Psuedomonas flourescens* diversity. Only background research and pilot tests were performed before the pandemic hit.

Additional Work History

Part-time Note Taker | Educational Equity at Penn State | State College, PA | 2022-current
Hornist | Pennsylvania Chamber Orchestra | State College, PA | 2023-current
Hornist | Nittany Valley Symphony | State College, PA | 2022-current
Hornist | Brandywiners Limited | Montchanin, DE | 2019-2022

Leadership and Activities

Primary chair (President) | Encore Benefiting THON | University Park, PA | 2021-current
Penn State Symphonic Wind Ensemble and Philharmonic Orchestra | University Park, PA | 2019-current
Penn State Chamber Orchestra | University Park, PA | 2022
Penn State Horn Society | University Park, PA | 2019-current